BIOCELL

Tech Science Press

http://doi.org/10.32604/biocell.2026.080282

ARTICLE

Dipeptidyl Peptidase 3 Knockdown in HeLa Cells Induces G0/G1 Cell Cycle Arrest Associated with Upregulation of p21 Protein

Lea Barbarić[1], Marina Oskomić[1], Anđela Horvat[2], Katja Ester[2], Nikolina Stojanović[3], Ana Tomašić Paić[1] and Mihaela Matovina[1,*]

[1]Division of Organic Chemistry and Biochemistry, Ruđer Bošković Institute, Zagreb, Croatia
[2]Division of Molecular Medicine, Ruđer Bošković Institute, Zagreb, Croatia
[3]Division of Molecular Biology, Ruđer Bošković Institute, Zagreb, Croatia
*Corresponding Author: Mihaela Matovina. Email: mmatovina@irb.hr

Received: 06 February 2026; Accepted: 27 April 2026; Published: 27 July 2026

ABSTRACT: Objectives: Dipeptidyl peptidase 3 (DPP3) is a zinc metallopeptidase involved in peptide turnover and possibly in blood pressure and pain regulation. It also modulates oxidative stress response via the Kelch-like ECH-associated protein 1–nuclear factor erythroid 2-related factor 2 (KEAP1–NRF2) pathway. Although frequently upregulated in cancer, its role in carcinogenesis remains unclear. This study examined the effects of DPP3 knockdown (KD) and overexpression on migration, proliferation, and KEAP1–NRF2 pathway regulation in HeLa cells. **Methods:** We assessed the effects of DPP3-KD and overexpression on HeLa cell migration using a wound healing assay, and on NRF2 activity by measuring mRNA levels of NRF2, NQO1, and CDKN1A (p21). Protein expression related to the regulation of the KEAP1–NRF2 pathway and cell proliferation was analyzed by western blot, and cell cycle distribution after DPP3-KD was analyzed by propidium iodide staining and subsequent analysis by flow cytometry. **Results:** We found that DPP3-KD in HeLa cells has no significant effect on the regulation of the KEAP1–NRF2 pathway in the basal conditions; however, it decreases cell migration ($^{*}p = 0.0123$) and induces G0/G1 arrest ($^{**}p = 0.0014$) associated with upregulation of p21 on both mRNA ($^{**}p = 0.0065$) and protein levels ($^{**}p = 0.0087$). Protein levels of cyclin A and cyclin E1 were decreased ($^{*}p = 0.037$ and $^{**}p = 0.0011$, respectively) in DPP3-KD, consistent with its effect on cell cycle distribution. **Conclusion:** Our results indicate that reduced proliferation of DPP3-KD HeLa cells is associated with upregulation of p21 and downregulation of cyclins A and E1. Investigation of the potential causal relationship between DPP3-KD and p21 upregulation was beyond the scope of this study.

KEYWORDS: Dipeptidyl peptidase 3; cyclin-dependent kinase inhibitor 1; kelch-like ECH-associated protein 1-nuclear factor erythroid 2-related factor 2 signaling; cell migration; G0/G1 arrest

1 Introduction

Dipeptidyl peptidase 3 (DPP3, DPP III; UniProt ID: Q9NY33) is a zinc metallopeptidase that sequentially cleaves dipeptides from the unsubstituted amino termini of peptides 3 to 10 amino acid residues in length. It displays broad substrate specificity, particularly for peptides containing 4 to 8 residues [1,2]. Although primarily considered a cytosolic enzyme, DPP3 has also been reported to associate with membranes [3] and the nucleus [4]. It is thought to participate in the final steps of intracellular protein turnover; however, DPP3 also shows *in vitro* activity towards several angiotensins [5,6], enkephalins [7,8], and endomorphins [7], indicating possible involvement in blood pressure regulation and pain modulation. More recently, DPP3 has

been identified as a biomarker of poor prognosis and potential therapeutic target in septic and cardiogenic shock, where it contributes to hemodynamic regulation via angiotensin II degradation [9].

Beyond the putative pathophysiological roles mediated by its peptidase activity, DPP3 also regulates the Kelch-like ECH-associated protein 1–nuclear factor erythroid 2-related factor 2 (KEAP1–NRF2) signaling pathway through interaction with KEAP1 [10]. The KEAP1–NRF2 pathway is the principal regulator of the cellular response to oxidative and electrophilic stress [11]. NRF2 is a transcription factor that controls the expression of more than 250 cytoprotective genes. Under basal conditions, NRF2 binds to KEAP1 in the cytoplasm and is rapidly degraded via the KEAP1-CUL3-RBX1 E3 ligase complex, which ubiquitinates NRF2, marking it for degradation by the 26S proteasome [12–14]. While NRF2 activity protects normal cells from carcinogenesis, constitutive NRF2 expression in established cancers promotes tumor survival through metabolic reprogramming and resistance to chemo- and radiotherapy [15]. Whether DPP3's involvement in KEAP1–NRF2 regulation is restricted to cancer, where DPP3 expression is frequently upregulated, remains unclear.

A role for DPP3 in cancer was suggested over two decades ago, when its elevated activity and abundance were found in endometrial carcinoma compared to normal tissue [16]. Similarly, increased DPP3 activity in malignant ovarian tissue correlated with tumor grade [17]. Subsequent studies confirmed upregulated DPP3 expression in squamous cell lung carcinoma [10] and breast cancer [18]. In a murine metastatic breast cancer model, DPP3 was among six signature genes predictive of breast cancer survival and lung cancer prognosis [19]. More recently, DPP3 overexpression in colorectal cancer correlated with lymph node metastasis, advanced pathological stage, and poor survival [20]. Elevated DPP3 mRNA [21] and protein levels have also been reported in esophageal cancer, where DPP3 protein overexpression is associated with the pathological stage and poor survival [22].

The mechanisms underlying the oncogenic effects of DPP3 overexpression are not fully understood. In estrogen receptor (ER)-positive breast cancer tissue, elevated DPP3 mRNA correlated with higher expression of 15 NRF2 target genes and poor survival [18]. Given NRF2's well-established role in carcinogenesis, enhanced NRF2 activity driven by DPP3 overexpression represents a plausible mechanism of cancer progression. However, NRF2-independent mechanisms are also likely. Notably, DPP3 has also been identified as a peptidase that reduces the antigenicity of necrotic tumor cells by degrading immunogenic peptides and inhibiting antigen cross-presentation [23], potentially allowing tumors to evade immune surveillance. Conversely, Tong et al. (2021) reported that DPP3 knockdown in HCT116 and RKO colorectal cancer cell lines inhibited cell growth, increased apoptosis, induced G2 arrest, reduced migration, and suppressed tumor growth *in vivo*. They attributed these effects to a newly identified interaction between DPP3 and CDK1; however, the mechanism by which this interaction accounts for all observed outcomes remains unclear [20].

Here, we aimed to analyze the effects of siRNA-mediated DPP3-KD and DPP3 overexpression, respectively, on cell migration, the KEAP1–NRF2 pathway regulation, and cell cycle progression in HeLa cells.

2 Materials and Methods

2.1 Cell Culture and Transfection

The HeLa cell line was a kind gift of Anamaria Brozović from Ruđer Bošković Institute, Zagreb, Croatia. The authenticity of HeLa cell line was confirmed by Cell Line Authentication analysis performed in Microsynth AG (Balgach, Switzerland). An in-house PCR test was used to confirm that cells are mycoplasma-free. HeLa cells were cultured in high-glucose Dulbecco's Modified Eagle Medium (DMEM with 4.5 g/L glucose; Sigma-Aldrich, St. Louis, MO, USA; Cat. No. D6429), enriched with 10% fetal bovine serum (FBS; Sigma-Aldrich, St. Louis, MO, USA; Cat. No. F9665), 1% non-essential amino acids (MEM

Non-essential Amino Acid Solution (100×); Sigma-Aldrich, St. Louis, MO, USA; Cat. No. M7145) and 1% antibiotic-antimycotic solution (Antibiotic/Antimycotic Solution (100×); Capricorn Scientific GmbH, Ebsdorfergrund, Germany; Cat. No. AAS-B). Cultures were maintained at 37°C in a humidified atmosphere with 5% CO_2.

Expression cDNA insert for DPP3 was cloned into the pFLAG-CMV2 vector as previously described [24]. Cells were seeded in 6-well plates at a density of 2×10^5 cells per well and grown to 70–90% confluency prior to transfection. For plasmid overexpression, cells were transfected with expression vectors encoding FLAG-DPP3 using DharmaFECT™ kb DNA transfection reagent (Dharmacon, Horizon Company, Lafayette, CO, USA; Cat. No. T-2006-01), according to the manufacturer's protocol. As a negative control, cells were transfected with the corresponding empty vector, pFLAG-CMV2. For gene silencing experiments, cells were transfected with 50 nM specific small interfering RNA (siRNA) targeting DPP3 (Ambion™ Silencer™ Select Pre-Designed siRNA; Thermo Fisher Scientific, Waltham, MA, USA; Cat. No. 4390824) using DharmaFECT™ 1 Transfection Reagent (Dharmacon, Horizon Company, Lafayette, CO, USA; Cat. No. T-2001-02), following the manufacturer's instructions. A non-targeting siRNA, siCTRL (Ambion™ Silencer™ Negative Control No. 2 siRNA; Thermo Fisher Scientific, Waltham, MA, USA; Cat. No. 4390846), was used as a negative control. Cells were collected 48–72 h post-transfection for RNA and protein isolation.

2.2 Wound Healing Migration Assay

For the wound healing assay, 3×10^5 cells were seeded into 6-well plates and grown to near confluency. Cells were transfected 24 h after seeding to either overexpress or knock down DPP3, depending on the experimental setup. The wound was created 48 h post-transfection. A sterile 200 µL pipette tip was used to create a straight scratch ("wound") across the monolayer. After washing twice with PBS (10 mM phosphate-buffered saline, pH = 7.4) to remove detached cells, fresh serum-free or low-serum medium was added to minimize proliferation effects. Images of the wound area were acquired immediately after scratching (0 h) and subsequently at defined time points (e.g., 20–22 h) using an inverted microscope Olympus IX50 (Olympus Optical Co., Ltd., Tokyo, Japan). The cell-free wound area was measured at each time point using ImageJ 1.54g software (NIH, Bethesda, MD, USA) (plug-in: Wound healing size tool). The degree of wound closure was quantified by calculating the cell-free area at each point relative to the initial area at 0 h. Statistical analyses were performed by two-way ANOVA with Bonferroni post-tests in GraphPad Prism 5.01 (GraphPad Software, Boston, MA, USA).

2.3 RNA Isolation and Quantitative Reverse Transcription-Polymerase Chain Reaction (RT-PCR)

Total RNA was extracted using the Direct-zol™ RNA MiniPrep Kit (Zymo Research, Irvine, CA, USA; Cat. No. R2050), following the manufacturer's instructions. RNA concentration and purity were measured using the BioDrop Duo spectrophotometer (Biochrom Ltd., Cambridge, UK). For cDNA synthesis, 1 µg of RNA was reverse-transcribed using the LunaScript™ RT SuperMix Kit (New England Biolabs, Ipswich, MA, USA; Cat. No. E3010S). Quantitative PCR was performed using Luna® Universal qPCR Master Mix (New England Biolabs, Ipswich, MA, USA; Cat. No. M3003L) on a CFX96 Real-Time PCR Detection System (Bio-Rad, Hercules, CA, USA). Gene-specific primers targeting NRF2, NQO1, and CDKN1A genes, and reference gene GAPDH were used (Table 1). The expression levels of NRF2, NQO1, and CDKN1A were normalized to GAPDH expression, which served as the internal reference gene. The analysis was performed in three biological replicates, and the results were analyzed using the Pfaffl method for relative quantification of RT-qPCR data, which takes into account the amplification efficiency of each gene [25].

Table 1: Primers used for qPCR.

Primer	Primer Sequence (5′→3′)	Product Size/pb	Reaction Efficiency	Ref.
GAPDH-FOR/REV	GAGTCAACGGATTTGGTCGT GACAAGCTTCCCGTTCTCAG	185	103.54	[26]
NRF2-FOR/REV	CACATCCAGTCAGAAACCAGTGG GGAATGTCTGCGCCAAAAGCTG	112	103.4	Origene primers
NQO1-FOR/REV	CCTGCCATTCTGAAAGGCTGGT GTGGTGATGGAAAGCACTGCCT	119	107.4	Origene primers
CDKN1A-FOR/REV	AGGTGGACCTGGAGACTCTCAG TCCTCTTGGAGAAGATCAGCCG	94	104.9	Origene primers

2.4 Protein Isolation and Western Blot Analysis

Proteins were isolated using RIPA lysis buffer (50 mM Tris-HCl (pH = 7.4), 150 mM NaCl, 1% NP-40, 0.5% sodium deoxycholate, 0.1% SDS). The buffer was supplemented with Halt™ Protease Inhibitor Cocktail (Thermo Fisher Scientific, Waltham, MA, USA; Cat. No. 78429). Cells were washed with cold PBS (10 mM phosphate-buffered saline, pH = 7.4), lysed on ice for 10 min, and centrifuged at 16,000× *g* for 20 min at 4°C to remove cellular debris. Equal amounts of total proteins were resolved by SDS-PAGE and transferred to nitrocellulose membranes. To ensure efficient protein transfer and verify equal loading across all lanes, total protein visualization was performed using Amido Black staining. Following electro transfer, nitrocellulose (NC) membranes (Amersham Protran Premium; Cytiva, Marlborough, MA, USA; Cat. No. 10600008) were stained with 0.1% (w/v) Amido Black 10B (Merck KGaA, Darmstadt, Germany; Cat. No. 1.01167) dissolved in a mixture of 2% (v/v) acetic acid and 10% (v/v) methanol for 5 min at room temperature with gentle agitation. This step served to simultaneously stain and fix the proteins to the membrane. To remove non-specific background staining, membranes were rinsed three times (2–3 min each) with a destaining solution (7% (v/v) acetic acid, 40% (v/v) methanol, and 53% (v/v) Milli-Q water) until dark-blue protein bands were clearly visible against a white background. After a brief rinse in deionized water, the NC membranes were scanned for densitometric analysis. Subsequently, membranes were rehydrated in Tris-buffered saline with 0.1% Tween-20 (TBST) for 30 min prior to blocking with 5% non-fat dry milk to prepare the surface for antibody incubation. After blocking with 5% non-fat dry milk in TBST (TBS with 0.1% Tween-20) for 1 h at room temperature, membranes were incubated overnight at 4°C with primary antibodies specific to the proteins of interest (FLAG-tag, DPP3, NRF2, NQO1, KEAP1, p62, p21, p27, cyclin A, and cyclin E1) (Table 2). Upon washing in TBST buffer, the membranes were incubated with the appropriate HRP-conjugated secondary antibodies for 1 h at room temperature. Specifically, conjugated goat anti-mouse IgG H&L secondary antibody (Abcam, Cambridge, UK; ab205719) or goat anti-rabbit IgG secondary antibody (Sigma-Aldrich, St. Louis, MO, USA; A6154) was used, both at a 1:10,000 dilution in 5% non-fat dry milk in TBST. Following secondary antibody incubation, the membranes were washed twice for 10 min in TBST and in TBS to remove residual detergent. Protein bands were visualized using Enhanced Chemiluminescence (ECL) reagents (Cytiva, Marlborough, MA, USA; RPN2109). Chemiluminescent signals were captured using the Alliance Q9 Mini imaging system (UVITEC, Cambridge, UK). Analysis was conducted using ImageJ 1.54g software (Bethesda, MD, USA). Band intensities (area under the curve) were normalized to Amido Black loading controls.

Table 2: Primary antibodies used in the study.

Antibody	Company	Dilution Ratio	Cat. No.
Anti-FLAG	Sigma-Aldrich, St. Louis, MO, USA	1:1000	F7425
Anti-DPP3 [EPR9021(B)]	Abcam, Cambridge, UK	1:10,000	ab133735
Anti-DPP3 polyclonal antibody		1:2000	ab217127
Anti-Nrf2 [EP1808Y]		1:500	ab62352
Anti-NQO1 [EPR3309]		1:5000	ab80588
KEAP1, monoclonal antibody	Proteintech, Rosemont, IL, USA	1:1000	60027-1-Ig
p21 polyclonal antibody		1:1000	28248-1-AP
P62/SQSTM1 polyclonal antibody		1:5000	18420-1-AP
Anti-cyclin A (B-8)	Santa Cruz Biotechnology, Santa Cruz, CA, USA	1:500	sc-271682
Anti-cyclin E (HE12)	Santa Cruz Biotechnology, Santa Cruz, CA, USA	1:1000	sc-247
Mouse Anti-p27 [Kip1] Clone 57/Kip1/p27 (RUO)	BD Biosciences, Franklin Lakes, NJ, USA	1:500	610242

2.5 Cell Cycle Analysis

At 48 h post-siRNA transfection, 1×10^6 cells were harvested by trypsinization using 0.1% trypsin and washed twice with ice-cold PBS (10 mM phosphate-buffered saline, pH = 7.4), by centrifugation at 260× *g* for 5 min. Cells were resuspended in 1.5 mL PBS and fixed by slowly adding 3 mL of ice-cold absolute ethanol drop-wise while vortexing. Fixed cells were incubated at −20°C overnight. After fixation, cells were washed twice with PBS by centrifugation at 260× *g* for 5 min at 4°C and resuspended in 100 µg mL^{-1} RNase A (Sigma Aldrich, St. Louis, MO, USA; Cat. No. R5503) in PBS. Following incubation at 37°C for 30 min, propidium iodide (Sigma Aldrich, St. Louis, MO, USA; Cat. No. P4170) was added to the final concentration of 25 µg mL^{-1}, and cells were incubated for 30 min on ice in the dark. DNA content was measured using a BD FACSymphony™ A1 flow cytometer (BD Biosciences, Franklin Lakes, NJ, USA). Data was recorded at a high flow rate, and 20,000 events per sample were acquired. Cell cycle distribution was analyzed using FCS Express 7 software (*De Novo* Software, Pasadena, CA, USA), and results are presented as percentages of cells in G0/G1, S, and G2/M phases.

2.6 Statistical Analysis

Statistical analyses were performed using GraphPad Prism 5.01 (GraphPad Software, San Diego, CA, USA). All experiments were performed in at least three biological replicates. Each biological replicate represents an independent experiment performed on HeLa cells at a different passage number, including independent transfection, cell lysis, and subsequent analyses. The results are displayed as mean +/− standard deviation (SD). Differences between two groups were assessed by an unpaired *t*-test (qPCR, western blot analysis), and differences among more than two groups were assessed by a two-way ANOVA with Bonferroni post-tests (cell migration and proliferation assays). Values of $p < 0.05$ were considered statistically significant.

3 Results

3.1 DPP3 Is Involved in the Regulation of HeLa Cell Migration

Despite several findings indicating that DPP3 has a role in the regulation of cell motility [20–22], the mechanism of DPP3's involvement in cell migration is largely obscure. Therefore, we investigated the role of DPP3 in regulating cell motility in HeLa cells. Wound-healing assays were performed in HeLa cells

following successful siRNA-mediated knockdown (Figs. 1A,B and S1) and plasmid-driven overexpression (Figs. 1C,D and S2) of DPP3, respectively. DPP3 knockdown (KD) significantly reduced wound closure compared to control siRNA, indicating impaired migratory capacity. Conversely, DPP3 overexpression significantly enhanced wound closure relative to the empty vector control, suggesting that elevated DPP3 levels promote migration. Together, these results demonstrate that DPP3 positively regulates migration in epithelial cancer cells.

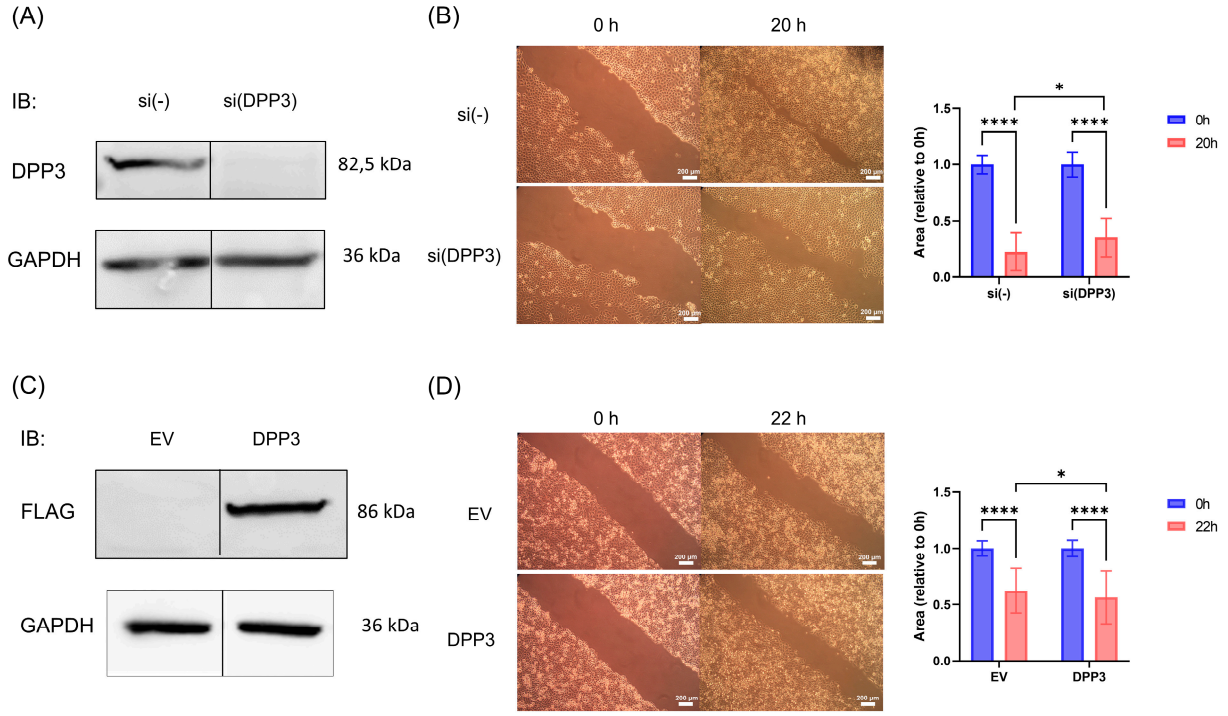

Figure 1: Wound-healing assay to determine the effect of DPP3 knockdown and overexpression, respectively, on HeLa cell migration. (**A**) Representative image of one of three biological replicates of western blot analysis of cell lysates from HeLa cells transfected with control siRNA (si(-)) or siRNA targeting DPP3 (si(DPP3)); (**B**) Representative image of one of three biological replicates of wound closure at 0 h and 20 h post-scratch of DPP3 siRNA silencing vs. si(-) control treated HeLa cells, respectively. The wound area before and after migration was determined using ImageJ software. Results were presented as mean ± SD of three independent biological replicates. Scale bar: 200 µm; images acquired at 10× magnification. Statistical analysis was performed using a two-way ANOVA with Bonferroni post-tests (*p = 0.0123; ****p < 0.0001); (**C**) Representative image of one of three biological replicates of western blot analysis of cell lysates from HeLa cells transfected with empty vector (EV) or FLAG-DPP3 (DPP3) expression construct; (**D**) Representative image of one of three biological replicates of wound closure at 0 h and 22 h of HeLa cells transfected with empty vector (EV) or FLAG-DPP3 (DPP3) expression construct. The wound area before and after migration was determined using ImageJ software. Results were presented as mean ± SD of three independent biological replicates. Scale bar: 200 µm; images acquired at 10× magnification. Statistical analysis was performed using a two-way ANOVA with Bonferroni post-tests (*p = 0.0375; ****p < 0.0001).

3.2 DPP3 Knockdown Induces the Expression of p21

Next, we analyzed the effect of DPP3-KD and overexpression on the mRNA expression of NRF2 itself and NQO1, as the most prominent NRF2-target gene. Considering DPP3-KD inhibits the growth of colorectal [20] and esophageal [21] cancer cell lines, we also included CDKN1A/p21 in our analysis to assess

potential effects of DPP3-KD on cell-cycle checkpoint regulation through the expression of p21, which is a representative cell-cycle checkpoint regulator downstream of stress-responsive signaling pathways [27]. Notably, CDKN1A is also a transcriptional target [28] and a competitive interactor of NRF2, which prevents its ubiquitination and consequently increases the activity of NRF2 [29]. Surprisingly, DPP3-KD in HeLa cells had no significant effect on the mRNA expression of NRF2 and NQO1 in the basal conditions; however, it upregulated the expression of CDKN1A (Fig. 2A).

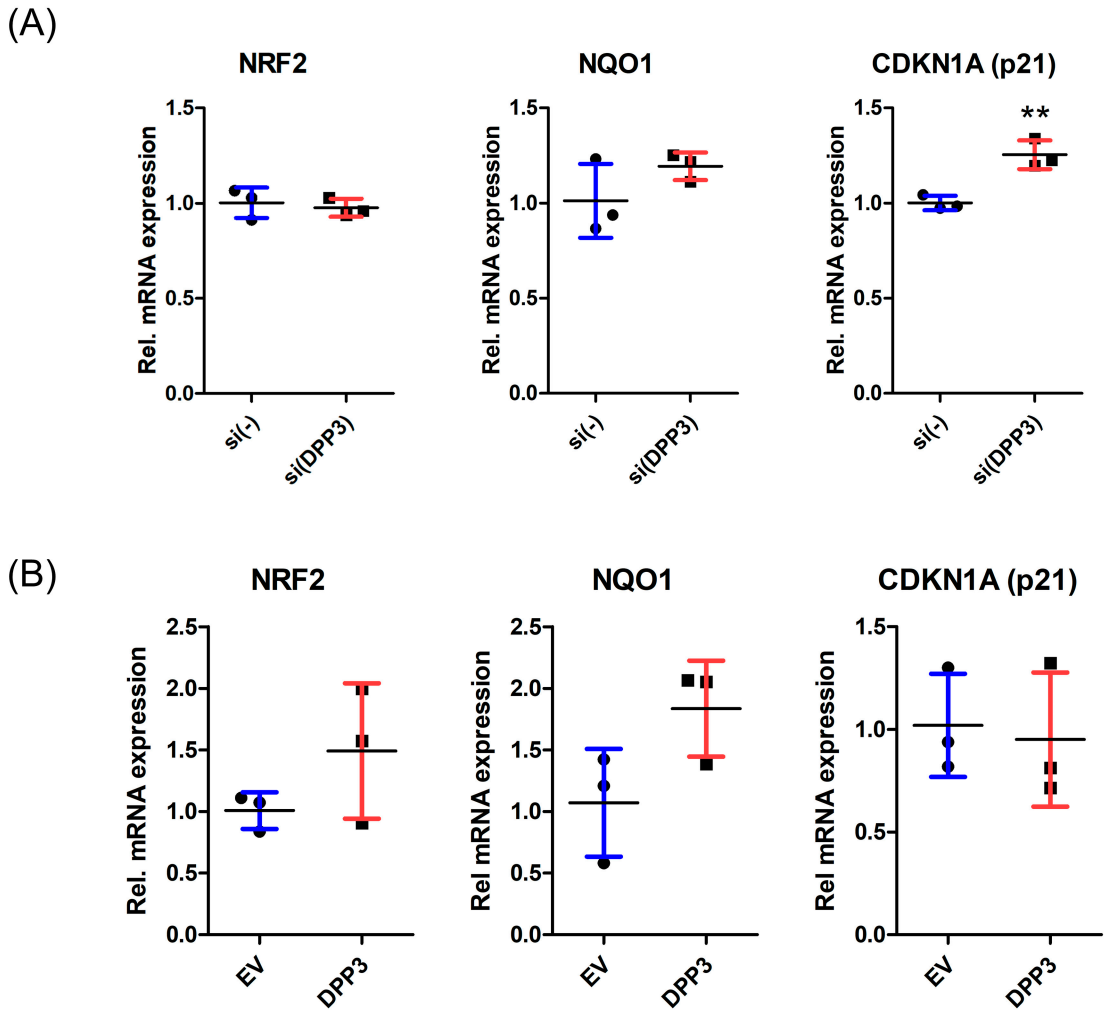

Figure 2: The effect of DPP3 knockdown and overexpression on the expression of NRF2-target genes. (**A**) Relative mRNA expression of NRF2, NQO1, and CDKN1A in cells with siRNA-mediated DPP3-KD (si(DPP3)) compared to negative control cells transfected with scrambled siRNA (si(-)); (**B**) Relative mRNA expression of NRF2, NQO1, and CDKN1A in cells transiently transfected with the pFLAG-CMV2-DPP3 vector (DPP3) compared to the empty vector control (EV). Gene expression was normalized to GAPDH. Data represent the mean ± SD of three biological replicates. Statistical analysis was performed using an unpaired *t*-test (**$p = 0.0065$).

FLAG-DPP3 overexpression upregulated mRNA expression of both NRF2 and NQO1, as would be expected, the difference in the expression was not statistically significant, while there was no effect on CDKN1A mRNA expression (Fig. 2B).

We also investigated the effect of DPP3-KD on protein levels of NRF2, NQO1, KEAP1, and p62, proteins involved in KEAP1–NRF2 signaling, and p21 protein, whose mRNA expression was upregulated in DPP3-KD

cells. We did not find a significant difference in the expression of NRF2, NQO1, KEAP1, or p62 in DPP3-KD HeLa cells (Figs. 3 and S3), confirming that DPP3-KD does not have a significant impact on NRF2 activity and NRF2-related proteins in HeLa cells under basal conditions. However, we found statistically significant upregulation of the p21 protein in DPP3-KD cells (Figs. 3 and S3).

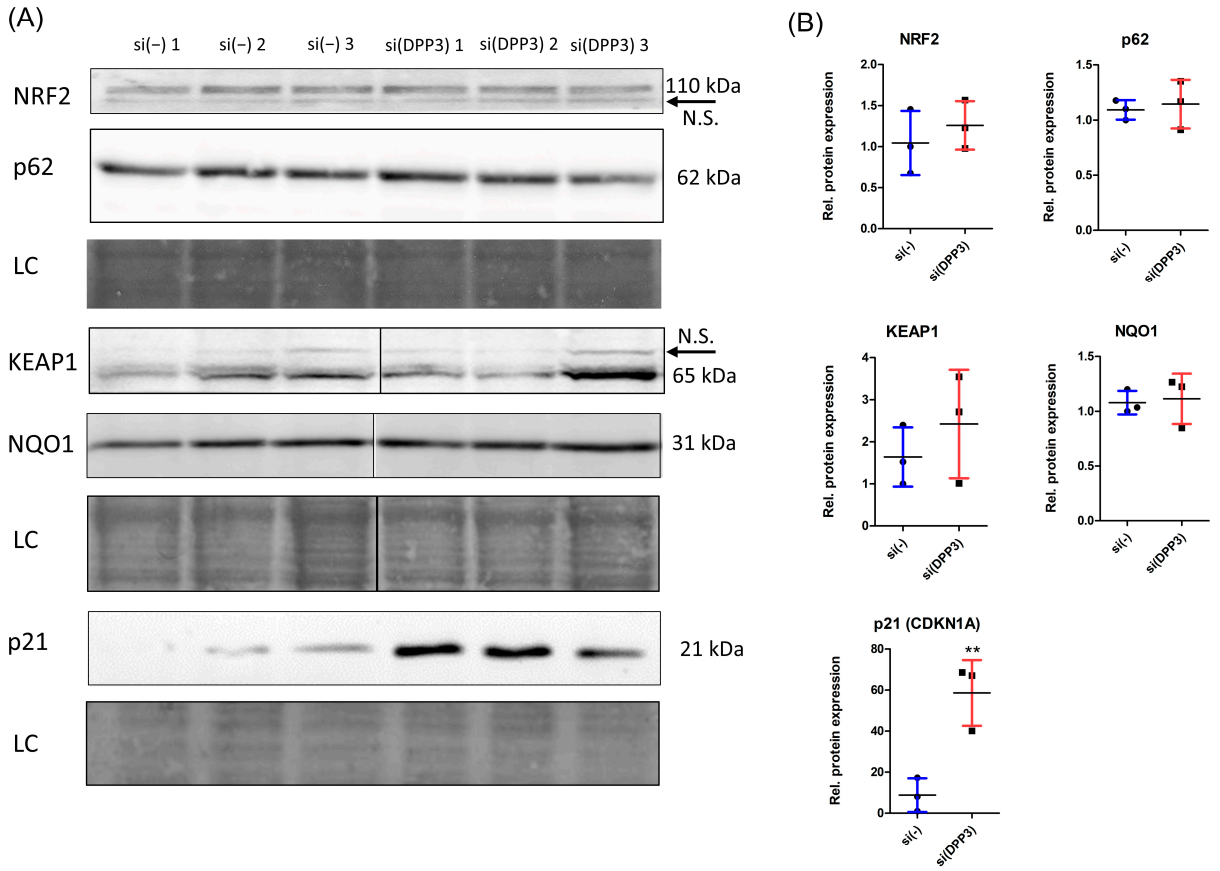

Figure 3: The effect of DPP3-KD in HeLa cells on the protein expression of NRF2, p62, KEAP1, NQO1, and p21. (**A**) Immunoblots of three biological replicates of negative control (si(-)) and DPP3-KD (si(DPP3)) are shown. Cells were harvested 48 h post-transfection. N.S.—non-specific bands. (**B**) Densitometric quantification of blots from A was normalized to total protein content using Amido Black staining (loading control, LC). Data represent the mean ± SD of three biological replicates. Statistical analysis was performed using an unpaired *t*-test (**$p = 0.0087$).

3.3 DPP3 Knockdown Induces G0/G1 Arrest in HeLa Cells

As we observed the upregulation of p21, an inhibitor of cell cycle progression upon DPP3-KD in HeLa cells, we decided to investigate whether DPP3-KD affects cell cycle dynamics. To this end, propidium iodide (PI)-stained HeLa cells were subjected to flow cytometric analysis following DPP3-KD. Flow cytometric analysis revealed clear differences in cell cycle phase distribution between control siRNA-transfected cells (si(-)) and cells transfected with siRNA against DPP3 (si(DPP3)) (Fig. 4A). Quantitative analysis showed that DPP3-KD significantly increased the proportion of cells in the G0/G1 phase, while the fraction of cells in the S phase decreased, but not statistically significantly (Fig. 4B). This shift indicates that depletion of DPP3 promotes G0/G1 cell cycle arrest, thereby impairing normal cell cycle progression.

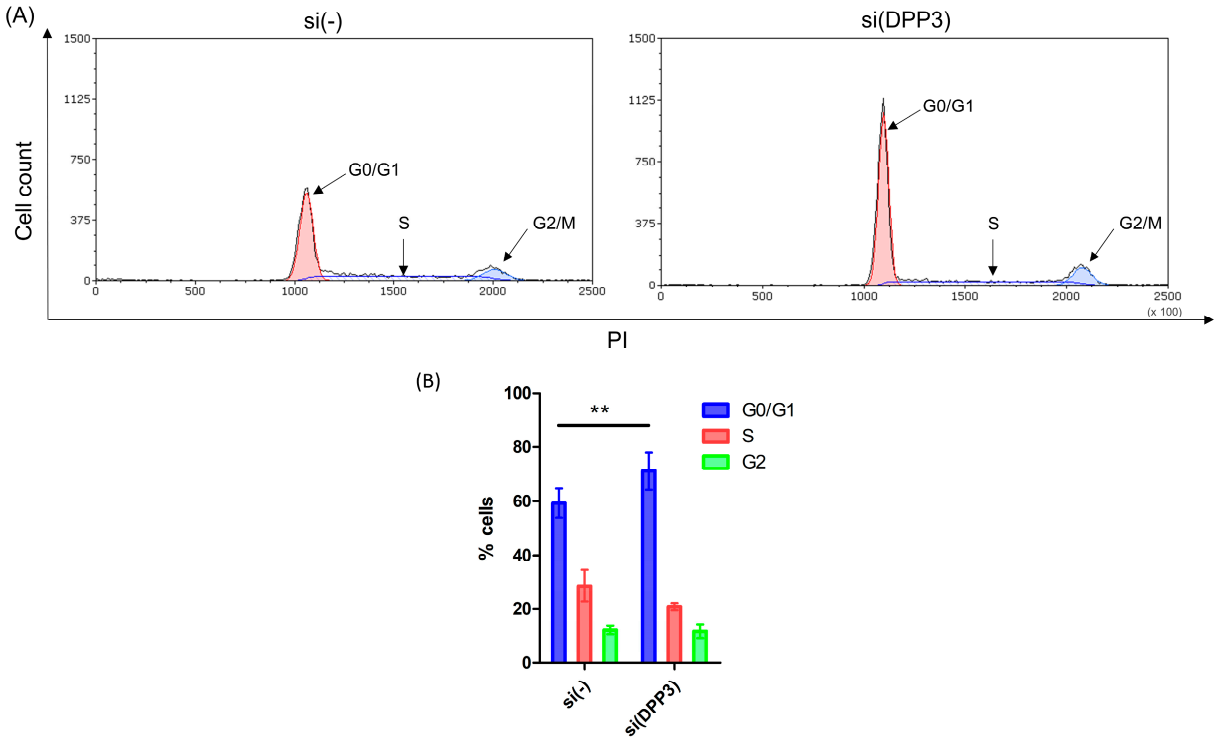

Figure 4: Flow cytometry cell cycle distribution analysis of control and DPP3-KD HeLa cells. (**A**) Representative histograms obtained by flow cytometry of control (si(-)) and DPP3-KD (si(DPP3)) HeLa cells. HeLa cells (si(-)) were harvested 48 h post-transfection. (**B**) Quantitative analysis of the percentage of cells within each phase was performed from at least 20,000 events per sample. Each bar represents the mean ± SD of the data obtained from four biological replicates. Statistical data analysis was performed by two-way ANOVA with Bonferroni post-tests. The difference in the G0/G1 phase of the cycle between si(-) and si(DPP3) treated cells was statistically significant (**p = 0.0014).

3.4 DPP3 Knockdown Decreases the Expression of Cyclins A and E1

Considering the observed effect of DPP3-KD on cell cycle progression and an increase in protein and mRNA expression of p21/CDKN1A, we analyzed the effect of DPP3-KD on protein levels of several additional proteins involved in the regulation of cell cycle, including cyclin A, cyclin E1, and cyclin-dependent kinase inhibitor p27. In line with the induction of G0/G1 arrest in DPP3 KD cells and strong upregulation of p21 protein levels, we found downregulation of cyclins A and E1, while there was no change in the expression of p27 (Figs. 5 and S4). As cyclins A and E1 are important for entry into S phase and cyclin A is also important for the further progression through S and G2 phase, these results corroborate that DPP3 might have a role in the regulation of proliferation of HeLa cells.

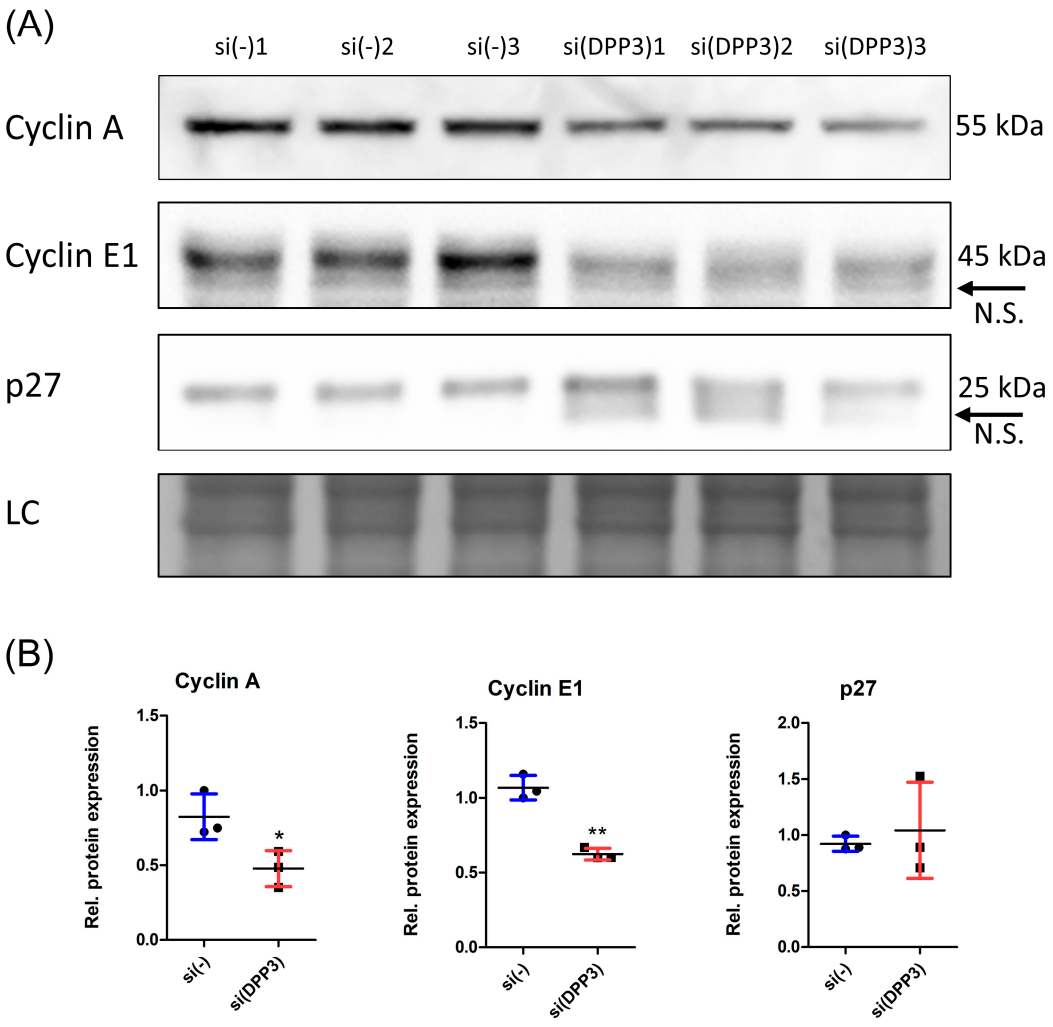

Figure 5: Western blot analysis of the effect of DPP3-KD in HeLa cells on the protein expression of cyclin A, cyclin E1, and p27. (**A**) Immunoblots of three biological replicates of negative control (si(-)) and DPP3-KD (si(DPP3)) are shown. N.S.—non-specific bands. (**B**) Densitometric quantification of all blots was normalized to total protein content using Amido Black staining (loading control, LC). Data represent the mean ± SD of three biological replicates. Statistical analysis was performed with an unpaired *t*-test (*p = 0.037; **p = 0.0011).

4 Discussion

We analyzed the effect of DPP3 knockdown (KD) and overexpression on HeLa cell migration and the regulation of the KEAP1–NRF2 signaling pathway, and the effect of DPP3-KD on HeLa cell proliferation. Our results, showing that DPP3-KD inhibits migration while DPP3 overexpression enhances it, are consistent with several other studies investigating the role of DPP3 in cell migration. In two colorectal cancer cell lines, HCT116 and RKO, shRNA-mediated DPP3-KD reduced malignant potential by downregulating proliferation and migration, upregulating apoptosis and apoptotic markers, and inducing G2 arrest. These effects were attributed to downregulation of CDK1 in DPP3-KD cells, mediated through a direct interaction between DPP3 and CDK1 [20]. Similarly, DPP3 depletion in several esophageal carcinoma cell lines inhibited proliferation and migration [21,22]. Interestingly, the impact of DPP3-KD on cell cycle progression varied between these models: in KYSE-410, Eca-109, and TE-1 cells, DPP3 depletion increased the proportion of cells in the S and G2 phases, whereas in TE-10 cells the pattern more closely resembled our findings in

HeLa cells, with an increased percentage of cells in G0/G1 and decreased S phase. These differences suggest that the effect of DPP3 on cell cycle regulation is most likely cell line dependent. Although the positive impact of DPP3 on cell migration and proliferation, together with its elevated expression in several cancers, is well established, the mechanisms underlying its role in migration remain unclear. Matovina et al. (2023) identified a novel, putative interactor of DPP3, SH2 domain-containing protein 3C (SH2D3C), a member of a protein family involved in cell migration and adhesion, and demonstrated that overexpressed proteins colocalize in membrane ruffles, structures important for cell migration, however, this interaction was not confirmed on endogenous proteins and it is not clear if DPP3's effect on cell migration might be mediated through its interaction with SH2D3C [30].

Surprisingly, DPP3 overexpression in HeLa cells had no effect on NRF2 or NQO1 mRNA expression under basal conditions. Similarly, DPP3-KD also did not affect NRF2 or NQO1 expression at either the mRNA or protein level in the basal conditions. This contrasts with previous reports showing that DPP3 overexpression enhances NRF2 activity via KEAP1 binding [10,18,24], and that DPP3 depletion decreases NRF2 activity in esophageal cancer cell lines KYSE-410 and TE-10, leading to downregulation of several NRF2 target genes, most notably NQO1, and reduced NRF2 and NQO1 protein levels in KYSE-410 cells [21]. Since DPP3 upregulates NRF2 through competitive binding to its inhibitor KEAP1, we also analyzed KEAP1 protein expression and found no difference in its levels. This prompted us to examine the expression of another competitive KEAP1 interactor, p62 (Sequestosome-1, SQSTM1), a well-established regulator of NRF2. p62 activates NRF2 through two mechanisms: by binding KEAP1 to block NRF2 ubiquitination [31], and by mediating KEAP1 degradation via autophagy [32]. Therefore, we analyzed p62 expression in DPP3-KD cells to determine whether p62 upregulation could compensate for DPP3 depletion; however, no difference in p62 protein expression was observed. Instead, we found that DPP3-KD significantly increased both mRNA and protein levels of cyclin-dependent kinase inhibitor p21. p21 regulates diverse cellular processes, including the cell cycle, DNA synthesis, stress response, apoptosis, and stem cell differentiation [27]. It was first identified in quaternary complexes with PCNA and cyclin D/CDK4, cyclin E/CDK2, cyclin A/CDK2, and cyclin B/CDC2, respectively; it inhibited kinase activity of the cyclin/CDK complexes, regardless of PCNA, and was, therefore, considered a universal inhibitor of cyclin-dependent kinases [33]. Later findings indicated that p21 preferably interacts with cyclin/cyclin-dependent kinase (CDK) complexes involved in the transition from G1 to S phase, and that p21 overexpression induces G1 arrest in human fibroblasts [34]. p21 expression is regulated mainly at the transcriptional level through p53-dependent and independent pathways [35]. p21 expression is also subjected to posttranscriptional regulation of its mRNA stability by miRNAs and RNA-binding proteins (RBPs), as well as the posttranslational regulation through phosphorylations and ubiquitinations that govern p21 protein stability, subcellular localization, and protein interactions [36]. In HeLa cells, p53 is inactivated by the interaction with HPV 18 E6 protein, which promotes its ubiquitin-mediated degradation [37]; therefore, upregulation of p21 in DPP3-KD HeLa cells has to be regulated through p53-independent pathways. Interestingly, p21 is a competitive interactor of NRF2 that competes with KEAP1 for the binding to NRF2's lower-affinity DLG motif and reduces NRF2 ubiquitination, thereby stabilizing NRF2 in colorectal carcinoma cells (HCT116) and in mouse models [29]. p21 is also a transcriptional target of NRF2 [28], so it is plausible that DPP3 KD in HeLa cells induces NRF2-dependant p21 upregulation, while p21 in turn binds NRF2 and prevents its degradation, compensating for the absence of DPP3.

Downregulation of cyclins A and E1 in DPP3-KD cells is also consistent with the accumulation of cells in G0/G1 phase, since both cyclins are involved in the transition from G1 to S phase of the cell cycle. Sequential activation of the cyclin D/CDK4/6, cyclin E/CDK2, and cyclin A/CDK2 drives the cells through G1

and S phases of the cell cycle [38]. Cyclin E accumulates at the G1/S boundary and forms active complexes with CDK2, while its inhibition blocks entry into S phase [39,40]. Cyclin A is required for the onset of DNA replication in mammalian fibroblasts [41,42] and HeLa cells [42]; however, it is also required for the transition from G2 to M phase of the cell cycle [42].

Herein, we demonstrate that DPP3-KD inhibits cell migration and induces G0/G1 arrest, accompanied by p21 upregulation and downregulation of cyclins A and E1. Investigation of the potential causal relationship between DPP3-KD and p21 upregulation was beyond the scope of this study; therefore, future studies are needed to elucidate the mechanisms underlying p21 upregulation, cyclins A and E1 downregulation, the potential role of p21 in NRF2 stabilization following DPP3-KD, and the pathways through which DPP3 regulates cell migration.

5 Conclusion

To our knowledge, we demonstrate for the first time that DPP3-KD induces the accumulation of cells in the G0/G1 phase of the cell cycle, accompanied by upregulation of p21 protein expression and downregulation of cyclins A and E1. These results could explain the inhibitory effect of DPP3-KD on cell proliferation found in several studies. Considering that cell cycle dysregulation is a common feature of cancer cells, identification of the potential new players involved in the control of the cell cycle might be important for the development of new therapeutic approaches. Our findings are especially interesting in light of frequent DPP3 overexpression found in several cancer types, including lung, breast, colorectal, and esophageal carcinoma. It is possible that DPP3 overexpression in these cancers is somehow connected to the deregulation of the cell cycle, through KEAP1–NRF2-dependent or -independent pathways.

Acknowledgement: None.

Funding Statement: The work was supported by the Croatian Science Foundation (CSF, https://hrzz.hr/en/) grant IP-2020-02-6743 awarded to Mihaela Matovina.

Author Contributions: Conceptualization, Mihaela Matovina; methodology, Mihaela Matovina, Anđela Horvat, Katja Ester and Nikolina Stojanović; validation, Mihaela Matovina, Anđela Horvat, Katja Ester and Nikolina Stojanović; formal analysis, Mihaela Matovina, Lea Barbarić, Marina Oskomić, Anđela Horvat and Nikolina Stojanović; investigation, Lea Barbarić, Marina Oskomić, Anđela Horvat and Ana Tomašić Paić; resources, Mihaela Matovina; writing—original draft preparation, Mihaela Matovina, Lea Barbarić and Marina Oskomić writing—review and editing, Mihaela Matovina, Lea Barbarić, Marina Oskomić, Anđela Horvat and Nikolina Stojanović; visualization, Mihaela Matovina, Lea Barbarić, Marina Oskomić, Anđela Horvat and Nikolina Stojanović; supervision, Mihaela Matovina; project administration, Mihaela Matovina; funding acquisition, Mihaela Matovina. All authors reviewed and approved the final version of the manuscript.

Availability of Data and Materials: The western blot data that support the findings of this study are available in Supplementary information (Figs. S1–S4) of this article. The original western blot figures are also included in the Supporting documents. Other data that supports the findings will be made available upon request.

Ethics Approval: Not applicable.

Conflicts of Interest: The authors declare no conflicts of interest.

Supplementary Materials: The supplementary material is available online at https://www.techscience.com/doi/10.32604/biocell.2026.080282/s1.

References

1. Karačić Z, Šupljika F, Tomić A, Brkljačić L, Paić AT, Ćehić M, et al. Neuropeptides, substrates and inhibitors of human Dipeptidyl peptidase III, experimental and computational study—A new substrate identified. Int J Biol Macromol. 2022;220:1390–401. [CrossRef].
2. Abramić M, Gruber K, Macheroux P, Tomić S. Dipeptidyl-peptidase III. In: Rawlings ND, Auld DS, editors. Handbook of proteolytic enzymes metallopeptidases. 4th ed. London, UK: Academic Press; 2025. p. 561–70. [CrossRef].
3. Malovan G, Hierzberger B, Suraci S, Schaefer M, Santos K, Jha S, et al. The emerging role of Dipeptidyl peptidase 3 in pathophysiology. FEBS J. 2023;290(9):2246–62. [CrossRef].
4. Sobočanec S, Filić V, Matovina M, Majhen D, Šafranko ŽM, Hadžija MP, et al. Prominent role of exopeptidase DPP III in estrogen-mediated protection against hyperoxia *in vivo*. Redox Biol. 2016;8:149–59. [CrossRef].
5. Jha S, Taschler U, Domenig O, Poglitsch M, Bourgeois B, Pollheimer M, et al. Dipeptidyl peptidase 3 modulates the renin–angiotensin system in mice. J Biol Chem. 2020;295(40):13711–23. [CrossRef].
6. Pang X, Shimizu A, Kurita S, Zankov DP, Takeuchi K, Yasuda-Yamahara M, et al. Novel therapeutic role for Dipeptidyl peptidase III in the treatment of hypertension. Hypertension. 2016;68(3):630–41. [CrossRef].
7. Baršun M, Jajčanin N, Vukelić B, Špoljarić J, Abramić M. Human Dipeptidyl peptidase III acts as a post-proline-cleaving enzyme on endomorphins. Biol Chem. 2007;388(3):343–8. [CrossRef].
8. Bezerra GA, Dobrovetsky E, Viertlmayr R, Dong A, Binter A, Abramić M, et al. Entropy-driven binding of opioid peptides induces a large domain motion in human Dipeptidyl peptidase III. Proc Natl Acad Sci U S A. 2012;109(17):6525–30. [CrossRef].
9. Ye P, Duan W, Leng YQ, Wang YK, Tan X, Wang WZ. DPP3: From biomarker to therapeutic target of cardiovascular diseases. Front Cardiovasc Med. 2922;9:974035. [CrossRef].
10. Hast BE, Goldfarb D, Mulvaney KM, Hast MA, Siesser PF, Yan F, et al. Proteomic analysis of ubiquitin ligase KEAP1 reveals associated proteins that inhibit Nrf2 ubiquitination. Cancer Res. 2013;73(7):2199–210. [CrossRef].
11. Suzuki T, Takahashi J, Yamamoto M. Molecular Basis of the KEAP1-NRF2 signaling pathway. Mol Cells. 2023;46(3):133–41. [CrossRef].
12. Cullinan SB, Gordan JD, Jin J, Harper JW, Diehl JA. The Keap1-BTB protein is an adaptor that bridges Nrf2 to a Cul3-based E3 ligase: Oxidative stress sensing by a Cul3-Keap1 ligase. Mol Cell Biol. 2004;24(19):8477–86. [CrossRef].
13. Zhang DD, Lo SC, Cross JV, Templeton DJ, Hannink M. Keap1 is a redox-regulated substrate adaptor protein for a Cul3-dependent ubiquitin ligase complex. Mol Cell Biol. 2004;24(24):10941–53. [CrossRef].
14. Kobayashi A, Kang MI, Okawa H, Ohtsuji M, Zenke Y, Chiba T, et al. Oxidative stress sensor keap1 functions as an adaptor for Cul3-based E3 ligase to regulate proteasomal degradation of Nrf2. Mol Cell Biol. 2004;24(16):7130–9. [CrossRef].
15. Dinkova-Kostova AT, Copple IM. Advances and challenges in therapeutic targeting of NRF2. Trends Pharmacol Sci. 2023;44(3):137–49. [CrossRef].
16. Šimaga Š, Babić D, Osmak M, Šprem M, Abramić M. Tumor cytosol Dipeptidyl peptidase III activity is increased with histological aggressiveness of ovarian primary carcinomas. Gynecol Oncol. 2003;91(1):194–200. [CrossRef].
17. Šimaga Š, Babić D, Osmak M, Ilić-Forko J, Vitale L, Miličić D, et al. Dipeptidyl peptidase III in malignant and non-malignant gynaecological tissue. Eur J Cancer. 1998;34(3):399–405. [CrossRef].
18. Lu K, Alcivar AL, Ma J, Foo TK, Zywea S, Mahdi A, et al. NRF2 induction supporting breast cancer cell survival is enabled by oxidative stress–induced DPP3–KEAP1 interaction. Cancer Res. 2017;77(11):2881–92. [CrossRef].
19. He M, Mangiameli DP, Kachala S, Hunter K, Gillespie J, Bian X, et al. Expression signature developed from a complex series of mouse models accurately predicts human breast cancer survival. Clin Cancer Res. 2010;16(1):249–59. [CrossRef].
20. Tong Y, Huang Y, Zhang Y, Zeng X, Yan M, Xia Z, et al. DPP3/CDK1 contributes to the progression of colorectal cancer through regulating cell proliferation, cell apoptosis, and cell migration. Cell Death Dis. 2021;12(6):529. [CrossRef].

21. Arora M, Kumari S, Kadian L, Anupa G, Singh J, Kumar A, et al. Involvement of DPP3 in modulating oncological features and oxidative stress response in esophageal squamous cell carcinoma. Biosci Rep. 2023;43(9):20222472. [CrossRef].
22. Liu JK, Abudula A, Yang HT, Xu LX, Nuerrula Y, Bai G, et al. DPP3 expression promotes cell proliferation and migration *in vitro* and tumour growth *in vivo*, which is associated with poor prognosis of oesophageal carcinoma. Oncol Rep. 2022;49(1):9. [CrossRef].
23. Gamrekelashvili J, Kapanadze T, Han M, Wissing J, Ma C, Jaensch L, et al. Peptidases released by necrotic cells control $CD8^+$ T cell cross-priming. J Clin Investig. 2013;123(11):4755–68. [CrossRef].
24. Matić S, Tomašić Paić A, Sobočanec S, Pinterić M, Pipalović G, Martinčić M, et al. Interdisciplinary study of the effects of Dipeptidyl-peptidase III cancer mutations on the Keap1-Nrf2 signaling pathway. Int J Mol Sci. 2022;23(4):1994. [CrossRef].
25. Pfaffl MW. A new mathematical model for relative quantification in real-time RT-PCR. Nucleic Acids Res. 2001;29(9):e45. [CrossRef].
26. Wang Q, Ma J, Lu Y, Zhang S, Huang J, Chen J, et al. CDK20 interacts with KEAP1 to activate NRF2 and promotes radiochemoresistance in lung cancer cells. Oncogene. 2017;36(37):5321–30. [CrossRef].
27. Elmitwalli O, Darwish R, Al-Jabery L, Algahiny A, Roy S, Butler AE, et al. The emerging role of p21 in diabetes and related metabolic disorders. Int J Mol Sci. 2024;25(23):13209. [CrossRef].
28. Jana S, Patra K, Jana J, Mandal DP, Bhattacharjee S. Nrf-2 transcriptionally activates P21Cip/WAF1 and promotes A549 cell survival against oxidative stress induced by H_2O_2. Chem Biol Interact. 2018;285:59–68. [CrossRef].
29. Chen W, Sun Z, Wang XJ, Jiang T, Huang Z, Fang D, et al. Direct interaction between Nrf2 and p21Cip1/WAF1 upregulates the Nrf2-mediated antioxidant response. Mol Cell. 2009;34(6):663–73. [CrossRef].
30. Matovina M, Tomašić Paić A, Tomić S, Brkić H, Horvat L, Barbarić L, et al. Identification of SH2 domain-containing protein 3C as a novel, putative interactor of Dipeptidyl peptidase 3. Int J Mol Sci. 2023;24(18):14178. [CrossRef].
31. Komatsu M, Kurokawa H, Waguri S, Taguchi K, Kobayashi A, Ichimura Y, et al. The selective autophagy substrate p62 activates the stress responsive transcription factor Nrf2 through inactivation of Keap1. Nat Cell Biol. 2010;12(3):213–23. [CrossRef].
32. Taguchi K, Fujikawa N, Komatsu M, Ishii T, Unno M, Akaike T, et al. Keap1 degradation by autophagy for the maintenance of redox homeostasis. Proc Natl Acad Sci U S A. 2012;109(34):13561–6. [CrossRef].
33. Xiong Y, Hannon GJ, Zhang H, Casso D, Kobayashi R, Beach D. p21 is a universal inhibitor of cyclin kinases. Nature. 1993;366(6456):701–4. [CrossRef].
34. Harper JW, Elledge SJ, Keyomarsi K, Dynlacht B, Tsai LH, Zhang P, et al. Inhibition of cyclin-dependent kinases by p21. Mol Biol Cell. 1995;6(4):387–400. [CrossRef].
35. Engeland K. Cell cycle regulation: p53-p21-RB signaling. Cell Death Differ. 2022;29(5):946–60. [CrossRef].
36. Dutto I, Tillhon M, Cazzalini O, Stivala LA, Prosperi E. Biology of the cell cycle inhibitor p21CDKN1A: Molecular mechanisms and relevance in chemical toxicology. Arch Toxicol. 2015;89(2):155–78. [CrossRef].
37. Lazo PA. The molecular genetics of cervical carcinoma. Br J Cancer. 1999;80(12):2008–18. [CrossRef].
38. Ju N, Zhao L, Yin S, Yang X, Zhou J, Gao J, et al. Cyclin-dependent kinases as therapeutic targets in cancer: Recent advances, challenges, and opportunities. Int J Cancer. 2026. [CrossRef].
39. Dulic V, Lees E, Reed S. Association of human cyclin E with a periodic G1-S phase protein kinase. Science. 1992;257(5078):1958–61. [CrossRef].
40. Ohtsubo M, Theodoras AM, Schumacher J, Roberts JM, Pagano M. Human cyclin E, a nuclear protein essential for the G1-to-S phase transition. Mol Cell Biol. 1995;15(5):2612–24. [CrossRef].
41. Girard F, Strausfeld U, Fernandez A, Lamb NJC. Cyclin a is required for the onset of DNA replication in mammalian fibroblasts. Cell. 1991;67(6):1169–79. [CrossRef].
42. Pagano M, Pepperkok R, Verde F, Ansorge W, Draetta G. Cyclin A is required at two points in the human cell cycle. EMBO J. 1992;11(3):961–71. [CrossRef].